

Annual variability of phytoplankton and bacteria in the subtropical North Pacific Ocean at Station ALOHA during the 1991-1994 ENSO event

LISA CAMPBELL, *‡ HONGBIN LIU,* HECTOR A. NOLLA* and DANIEL VAULOT†

(Received 13 November 1995; in revised form 31 May 1996; accepted 5 October 1996)

Abstract—Time-series data on community structure in the upper 200 m at Station ALOHA in the subtropical North Pacific were collected at approximately monthly intervals from December 1990 through to March 1994 during an extended El Niño-Southern Oscillation (ENSO) event. Samples were analyzed by flow cytometry to enumerate *Prochlorococcus*, *Synechococcus*, picoeucaryotes, 3 - 20 µm algae, and heterotrophic bacteria, as well as to quantify cellular chlorophyll fluorescence for the autotrophic components. A significant seasonal cycle was evident in cellular chlorophyll fluorescence for each of the autotrophic components, with maxima occurring each winter as a consequence of photoacclimation. Abundance of each picophytoplankton component exhibited temporal variability on both seasonal and interannual scales. Although the magnitude of the seasonal cycles in the abundance was relatively small, the cycles appeared to be out of phase. Typically, abundance maxima of *Synechococcus* occurred in winter, of picoeucaryotes in spring, and of *Prochlorococcus* during summer/fall. The different timing in these cycles may explain why the presence of a seasonal pattern in total phytoplankton biomass has been difficult to establish. Abundance of the larger 3-20 µm algae varied over two orders of magnitude during the time series, with no obvious seasonal pattern. The 3 - 20 µm algae were a small percentage of the total estimated carbon biomass (~ 8 %). Heterotrophic bacteria were the most numerous of the picoplankton and the seasonal pattern in their 200-m integrated abundance paralleled *Prochlorococcus* over the time series. Together, the procaryotes contributed 60 - 90 % of the total estimated microbial carbon. Significant interannual variation in the total 200-m integrated microbial carbon estimates may be related to the effects of the extended ENSO event which began in 1991. © 1997 Elsevier Science Ltd. all rights reserved.

INTRODUCTION

The subtropical central North Pacific Ocean has been described as homogeneous with respect to its physical and biological properties. Previous studies reported the central gyre to be a stable community, and stochastic events were proposed to explain the observed variability in phytoplankton biomass (e.g. McGowan and Hayward, 1978; Hayward *et al.*, 1983; DiTullio and Laws, 1991). Documented variations in primary production and biomass were small (e.g., Bienfang and Szyper, 1981), with no discernible seasonal cycle.

More recent reports, however, provide evidence that seasonal variation in phytoplankton

*Department of Oceanography, School of Ocean and Earth Science and Technology, University of Hawaii, Honolulu, HI 96822, U.S.A.

†Station Biologique, CNRS, INSU, Université Pierre et Marie Curie, BP 7r, 29682 roscoff Cédex, France.

‡Present address: Department of Oceanography, Texas A&M University, College Station, TX 77843-3146, U.S.A.

biomass in the subtropical North Pacific does exist. At the Hawaiian Ocean Time series (HOT) Station ALOHA (22°45' N; 158° W), seasonal cycles have been observed in chlorophyll *a* (chl *a*) concentrations at the depth of the chl maximum layer (Letelier *et al.*, 1993) and in the depth of the nitracline (Dore and Karl, 1996). Winn *et al.* (1996) also found significant seasonal variations in *in situ* fluorescence and chl *a* concentrations at Station ALOHA, but the cycles differed in the upper and lower portions of the euphotic zone. In the upper 50 m, the winter increase in chl *a* concentration was found to be a photoadaptive response to the lower average light intensities experienced by the phytoplankton in the mixed layer, and was not the result of an increase in phytoplankton biomass. In the lower euphotic zone, however, the seasonal maximum in chl *a* concentration in May or June was due to a change in the rate of primary production and in phytoplankton biomass as a consequence of increased light intensity in summer. Venrick (1993) examined 17 years of data for the central North Pacific at 31°N and found seasonal cycles in the phytoplankton community structure. Although seasonal maxima in surface species and deep species are evident, the cycles are independent, thus the seasonal cycle in biomass is obscured.

Interannual variations in community structure have been reported by Blanchot *et al.* (1992) for the western equatorial Pacific between the 1987 ENSO event and the subsequent non-ENSO conditions in 1988. Under nitrate-limited conditions, the smaller cells (<1 μm) contributed > 60 % of chl *a*; however, in a normal year, when nitrate is present, or at depths where nitrate was not limiting, the larger cells predominated. More recently, Karl *et al.* (1996) attributed a major change in structure and productivity of the pelagic ecosystem in the subtropical North Pacific Ocean at Station ALOHA to the ENSO event of 1991/1992. They found a substantial increase in primary production and assimilation number ($\text{mg C mg Chl a}^{-1} \text{h}^{-1}$) between the 1989/1990 pre-ENSO and 1991/1992 ENSO time periods. The average surface (0–50 m depth interval) productivity in 1989/90 was < 5 $\text{mg C mg chl a}^{-1} \text{hr}^{-1}$. But between 1991 and 1992, productivity increased to > 5 $\text{mg C mg chl a}^{-1} \text{hr}^{-1}$ and varied as a logarithmic function of the mixed-layer depth. During this period the water column became more stable, as the frequency of mixed-layer depths ≥ 60 m decreased (Letelier *et al.*, 1996). Significant variations in phytoplankton biomass have also been observed on a longer, decadal time scale. From a > 20-year time series, Venrick *et al.* (1987) reported a significant increase in chl *a* since 1970, which was coincident with interdecadal sea surface temperature (SST) and atmospheric circulation anomalies. The interdecadal SST warming in the tropical Pacific, concurrent with SST cooling in the mid latitudes, and a deepening of the Aleutian Low developed quite rapidly in the late 1970s (Wang, 1995).

The microbial community structure in the euphotic zone of the subtropical Pacific at Station ALOHA is dominated by procaryotes, in particular *Prochlorococcus* (Campbell *et al.*, 1994). However, the dynamics of the picoplankton community have not been examined. The goal of our project was to examine time series abundance data from Station ALOHA to elucidate the scales in temporal variability in the structure and composition of the picophytoplankton community.

METHODS

Sample collection and enumeration

Samples from Station ALOHA (Fig. 1) were collected at approximately monthly intervals

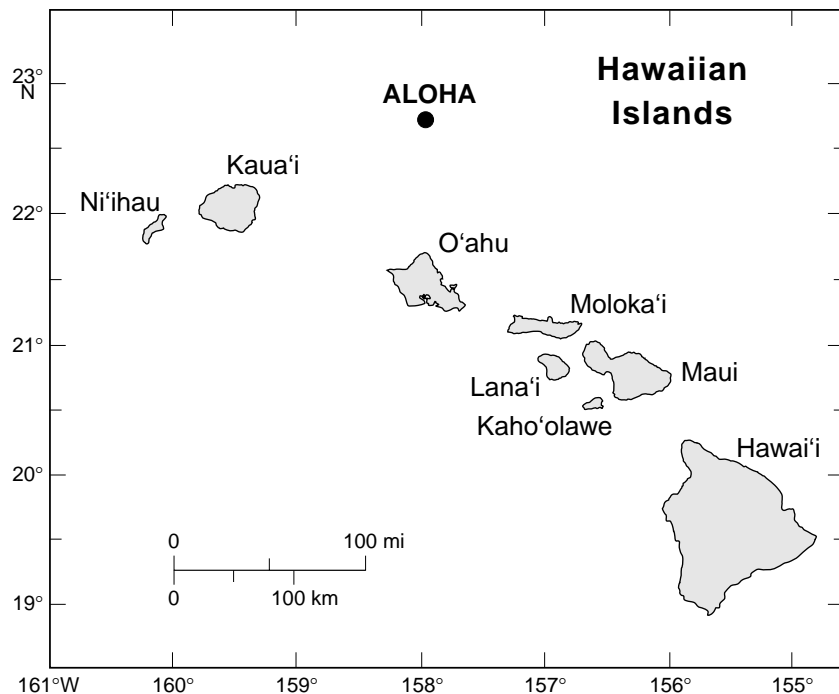


Fig. 1. Location of Station ALOHA, 100 km north of Oahu, HI.

from 12 depths within the upper 200 m water column using Niskin bottles attached to a SeaBird (model SBE-09) CTD rosette system (Karl and Winn, 1991). To remove the effect of diel variations in abundance and cellular fluorescence, effort was made to collect all samples around midnight, by which time most cells have completed cell division (e.g. Vaultot *et al.*, 1995; Campbell, unpubl.). This was mostly successful in that 27 of the 31 profiles were collected between 2100 and 0300. Two profiles (Aug 1991 and May 1992) were collected at 2000 h, and only two profiles were taken during daylight hours (April 1991 and Nov 1992; at 1000 and 1630 h, respectively). Thus, midday samples, in which fluorescence would be most adversely affected, were largely avoided.

For picoplankton, samples were preserved with paraformaldehyde (0.2% final concentration), quickly frozen in liquid nitrogen and stored at -80°C until analysis (Vaultot *et al.*, 1989). This method has been used successfully for picoplankton and larger phytoplankton species (Vaultot *et al.*, 1989; Olson *et al.*, 1990; Simon *et al.*, 1994). In an independent comparison of our protocol with epifluorescence microscopy, close agreement between the two methods was obtained for picoplankton abundance (Buck *et al.*, 1996). For the larger algae, samples from the first year (Dec 90- Sept 91) were preserved and frozen in four 15-ml aliquots, as above. All subsequent samples were preserved and stored at 4°C until analysis (within 48 hrs), as previously reported (Campbell *et al.*, 1994).

To enumerate each component of the plankton, flow cytometry analyses were conducted using high sensitivity modifications as previously described (Olson *et al.*, 1990, Campbell

and Vaultot 1993; Campbell *et al.*, 1994). For the picoplankton, *Prochlorococcus*, *Synechococcus*, picoeucaryotes, sample volumes were 100 - 200 μl . For heterotrophic bacteria, 250 μl samples were stained with Hoechst 33342 (1 $\mu\text{g}/\text{ml}$), as described previously (Campbell *et al.*, 1994), and 100 μl enumerated. Our results most likely include the non-nucleoid containing cells noted by Zweifel and Haagstrom (1995). However, to remain consistent with all previous reports of heterotrophic bacteria, we report our total Hoechst-stained counts (corrected for *Prochlorococcus*, as permitted by dual beam flow cytometry) as heterotrophic bacteria. For the 3 - 20 μm algae, sample volumes ranged from 50 - 200 ml and were processed using the modifications of Olson *et al.* (1989). Mean counts for the 3 - 20 μm analyses ranged from 50 to several 1000 events. All chlorophyll fluorescence data (exc. 488 nm, em. 680 nm) for picoplankton and larger algae were normalized to 0.57 μm yellow-green Fluoresbrite beads (Polysciences), which permitted us to make comparisons of chl fluorescence among cruises for each group. Preservation by fixation and freezing in liquid nitrogen is satisfactory for most picoplankton (Vaultot *et al.*, 1989; Olson *et al.*, 1990; Simon *et al.*, 1994). Preservation may lead to an increase in chl fluorescence signal (e.g., Simon *et al.*, 1994), but this is variable and dependent on species examined. All flow cytometry data were collected in list mode and transferred to a PC for analysis by CYTOPC (Vaultot 1989).

Nutrient, CTD, and other hydrographic data were obtained from the Hawaii Ocean Time Series data base (Winn *et al.*, 1993; Tupas *et al.*, 1993, 1994, 1995) available by anonymous ftp (mana.soest.hawaii.edu in the /pub/hot directory). The mixed layer depth was defined as the shallowest depth where the density gradient was $\geq 5 \text{ g m}^{-4}$. For $\text{NO}_3 + \text{NO}_2$, the limit of detection was 2 nM, with a precision and accuracy of $\pm 1 \text{ nM}$ (Tupas *et al.*, 1995). The nitracline was defined as the shallowest depth for the first appearance of 0.1 μM $\text{NO}_2 + \text{NO}_3$ and was calculated as in Winn *et al.* (1996). The depth of the deep chl maximum layer (DCML) was determined by in situ flash fluorometry (Winn *et al.*, 1996). Monthly wind speed data and anomalies (m s^{-1}) were obtained from the *Climate Diagnostic Bulletin*. Conditions were categorized as normal (NE trades), stronger than normal trades, or weaker than normal trades based on difference from the 1961-1983 composite (B. Wang, personal communication, 1996).

Seasonal and interannual variations

To examine seasonal and interannual variations in community structure and composition, data from profiles for each cruise were contoured using Surfer for Windows (Golden Software, Inc.) with the kriging gridding method. All sample depths were normalized to the individual cruise mean density profiles to minimize the effect of internal waves.

Carbon biomass estimates

Biomass estimates were made using the carbon conversion factors applied previously for Station ALOHA (Campbell *et al.*, 1994): 53 fg C cell⁻¹ for *Prochlorococcus*, 250 fg C cell⁻¹ for *Synechococcus*, and 20 fg C cell⁻¹ for heterotrophic bacteria. For the eucaryotic algae, we used the relationship $\text{pg C} = 0.433 \times (\text{biovolume})^{0.866}$, and average cell volumes were 6.22 μm^3 for picoeucaryotes and 370 μm^3 for 3- 20 μm algae.

Interannual differences in 200-m integrated abundance and carbon biomass for each

component and total microbial carbon were tested for significance by the nonparametric Kruskal-Wallis method. The significance of differences of average abundances between pairs of years was determined by the Kolmogorov-Smirnov test.

RESULTS

Flow cytometric analyses of community structure in the subtropical North Pacific at Station ALOHA over a 40-month period (December 1990–March 1994) provide the basis for a descriptive summary of spatial and temporal distributions of the microbial populations. We present (i) characteristic vertical profiles of abundance and cellular chl fluorescence for each component; (ii) time series of cellular chlorophyll fluorescence for each photosynthetic component; (iii) time series of abundances for each group; and (iv) the interannual variations in abundance and carbon biomass.

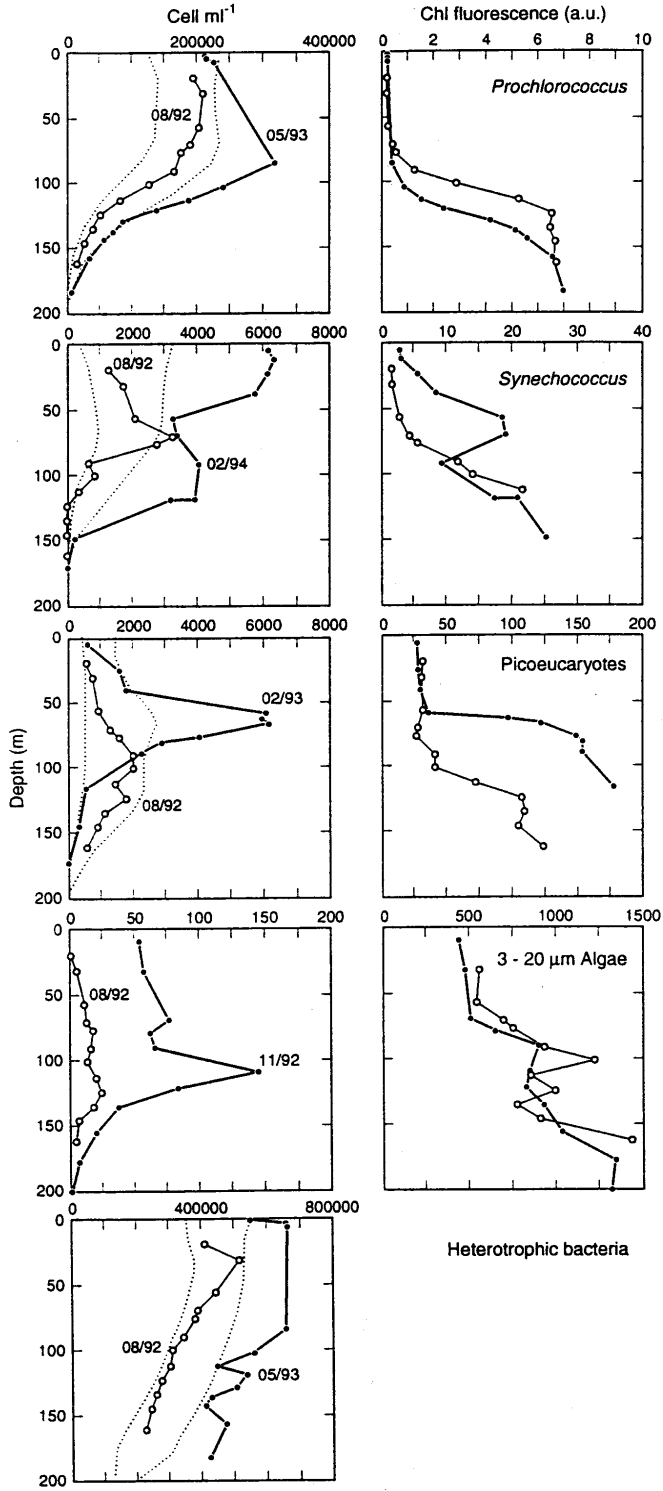
Vertical distributions of abundance

Prochlorococcus is the numerically dominant autotrophic component of the microbial community at Station ALOHA. The abundance of *Prochlorococcus* was fairly uniform above 100 m where the median count was 176×10^3 cell ml⁻¹, but decreased rapidly down to a median value of 6.6×10^3 cell ml⁻¹ by 150 - 200 m. A characteristic profile (August 1992) and maximum abundance profile are plotted in Figure 2. The overall variation during this three-year time series was small, which is indicated by the overlaid curves showing ± 1 SD of the mean of all profiles for the 40-month sampling period ($n = 31$). The SD plots were smoothed by the distance-weighted least squares smoothing function (Systat, Inc., Evanston, IL). The maximum in *Prochlorococcus* cell abundance often occurred below the surface mixed layer (average depth 76 ± 23 m), and ranged two-fold from $1.4 - 3.2 \times 10^5$ cell ml⁻¹ (Fig. 2).

Synechococcus is less important numerically than *Prochlorococcus* and is generally restricted to the upper 100 m, where the median abundance was 1.4×10^3 cell ml⁻¹ (Fig. 2). Maxima in abundance occurred at 75 m (± 25 m) and ranged 6- fold over the time series, from $1.1 - 6.3 \times 10^3$ cell ml⁻¹. The variability of *Synechococcus* abundance was greatest in the upper 50 m. During winter months, *Synechococcus* extended deeper in the water column (Fig. 2); consequently, *Synechococcus* integrated abundance had the most pronounced seasonal pattern (see below).

The picoeucaryotes, small ($<3 \mu\text{m}$) eucaryotic algae, occurred at abundances similar to *Synechococcus*. Median abundance in the upper 100 m was 1.0×10^3 cell ml⁻¹. The vertical profile of picoeucaryotes displayed a subsurface maximum (median depth $111 \text{ m} \pm 22 \text{ m}$, Fig. 2), which ranged from 0.7×10^3 cell ml⁻¹ in Aug 1991 to 6.2×10^3 cell ml⁻¹ in April 1993, an overall 9-fold range during the entire time series. The subsurface peak in picoeucaryote abundance occurred close to the DCML (Fig. 3) and the correlation between the depths of the subsurface maximum and the DCML was significant (0.51 ; $p < 0.01$). At times the peak in picoeucaryote abundance was quite shallow, e.g. Feb 93, when the peak coincided with a nitracline and DCML that were also shallower than usual (Figs. 2 & 3).

The 3–20 μm diameter algae were distinguished by their scatter and chlorophyll fluorescence flow cytometric signals, which were much larger than those of the picoeucaryotes. The typical vertical profile of the 3–20 μm algae (Fig. 2) was similar to



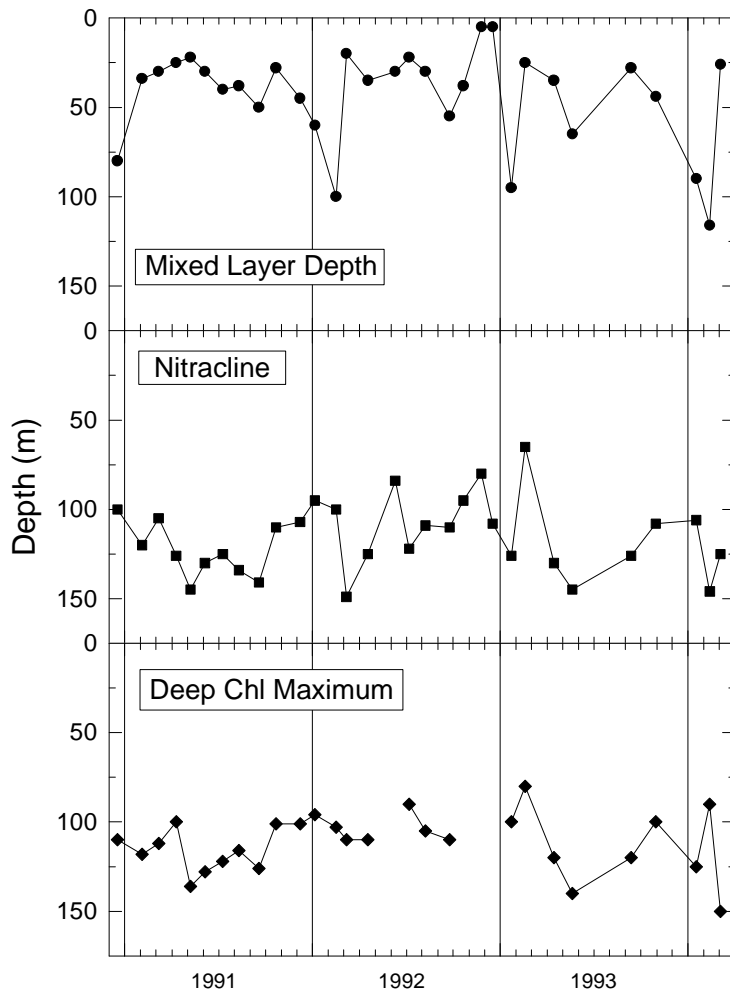


Fig. 3. Surface mixed layer and nitracline depths (after Winn *et al.*, 1996 and additional data), and fluorescence maximum depths (after Letelier *et al.*, 1993 and additional data from HOT data base).

Fig. 2. Vertical profiles of abundance for *Prochlorococcus*, *Synechococcus*, picoeucaryotes, larger algae, and heterotrophic bacteria, and cellular chlorophyll fluorescence normalized to 0.57 μm YG Fluoresbrite beads (Polysciences, Inc.) for photosynthetic components of the microbial community at Station ALOHA in the subtropical North Pacific. All depths are normalized to cruise mean density profiles to minimize the effect of internal waves. A typical profile (from August 1992) and the maximum abundance profile during the time series are plotted for each component. Also plotted are the curves for ± 1 SD of 3-yr mean profile (fitted by distance-weighted least squares smoothing of the means of 5 m-interval binned data from all 31 cruises [Systat, Inc., Evanston, IL]). First row: *Prochlorococcus* typical (August 1992) and maximum (May 1993) profiles with ± 1 SD; chl fluorescence cell^{-1} for August 1992 and May 1993. Second row: *Synechococcus* typical (August 1992) and maximum (February 1994) profiles with ± 1 SD; chl fluorescence cell^{-1} for August 1992 and February 1994. Third row: Picoeucaryotic algae typical (August 1992) and maximum (February 1993) profiles with ± 1 SD; chl fluorescence cell^{-1} for August 1992 and February 1993. Fourth row: The 3–20 μm chl-fluorescing algae typical (August 1992) and maximum (November 1992) profiles; The coefficient of variation for each 5m-bin was $\sim 100\%$, so curve fitting for SD could not be resolved; chl fluorescence cell^{-1} for August 1992 and November 1992. Fifth row: Heterotrophic bacteria typical (August 1992) and maximum (May 1993) profiles with ± 1 SD.

the picoeucaryotes in that a subsurface maximum (average depth $111 \text{ m} \pm 27 \text{ m}$) occurred at or just below the deep chl maximum. Peaks in abundance ranged from 3–144 cell ml^{-1} . Both the fixation procedure and the sample volume are likely inadequate for some of the algal species (Vaulot *et al.*, 1989; Lepesteur *et al.*, 1993), therefore, abundance is liable to be underestimated. Still, the 3–20 μm algae are small percentage of the total biomass (see below).

Heterotrophic bacteria (i.e., non-chlorophyll containing procaryotes) were enumerated by dual-beam flow cytometry to distinguish them from *Prochlorococcus*, which contribute a significant percentage of the total procaryotic cell counts (Campbell *et al.*, 1994). During this time series, *Prochlorococcus* contributed 28 % (± 6.3 %) of the total procaryotic cell counts in the upper 100 m, which is similar to the 31 % reported previously (Campbell *et al.*, 1994). Vertical profiles of heterotrophic bacteria abundance were quite uniform in the upper 150 m, but typically the maximum abundance occurred in the surface mixed layer with a median value of 4.2×10^5 cell ml^{-1} (range $2.3 - 7.4 \times 10^5$ cell ml^{-1}). Abundance decreased slowly to a median value of 2.2×10^5 cell ml^{-1} (range $0.9 - 5.2 \times 10^5$ cell ml^{-1}) below 150 m (Fig. 2).

Cellular chlorophyll fluorescence

Cellular chl fluorescence, or the mean fluorescence per cell, which is an index of cellular chl *a* concentration, increased with depth for all photosynthetic components of the community. The vertical profile for *Prochlorococcus* chlorophyll fluorescence appeared as two layers of constant cellular fluorescence (low fluorescence in the surface mixed layer; high fluorescence in the deeper layer) which were separated by a sharp gradient (Fig. 2). The average increase in cellular chl fluorescence between the low fluorescence and the high fluorescence layers was 35 (± 14 SD) times (e.g., Fig 2); the maximum observed increase was almost 80-fold. Based on our 40-month time-series, we observed a seasonal pattern in average cellular fluorescence throughout the upper 100 m (Fig. 4). In the upper portion of the water column, seasonal variation is two-fold, with a maximum in winter. In the deeper portion of the euphotic zone (below 100 m), the seasonal cycle is less pronounced (see also Winn *et al.*, 1996).

Cellular chl fluorescence for *Synechococcus* also increased with depth, although the deeper high fluorescence layer was restricted due to the abrupt decrease of cells below 100 m. Maximum fluorescence was 20 (± 14 SD) times higher than in the low fluorescence surface layer; the maximum increase was 60-fold. Based on fluorescence emission (525: 575) and excitation (488: 457-515) ratio indexes (Campbell and Vaulot, 1993), the increase in cellular fluorescence with depth appeared to be predominately due to an increase in chl per cell, not a succession of *Synechococcus* strains with different phycoerythrin pigment types (e.g., dims vs. brights, Olson *et al.*, 1990). The 488 : 457-515 excitation ratio showed a slight increase with depth (1.9 vs 2.2) but these values are within the range reported for strains with a high phycourobilin: phycoerythrobilin (PUB:PEB) chromophore composition. For *Synechococcus* which lack PUB, or have low PUB:PEB ratios, the fluorescence excitation ratios are closer to 1.0 (Campbell and Vaulot, 1993). Values remained at ~ 2.0 , with no indication of seasonal variation.

The average cellular chl fluorescence for *Synechococcus* in the upper portion of the euphotic zone displayed a significant seasonal cycle, with a winter maximum; however, because *Synechococcus* was often absent below 100 m, statistical analysis was not possible

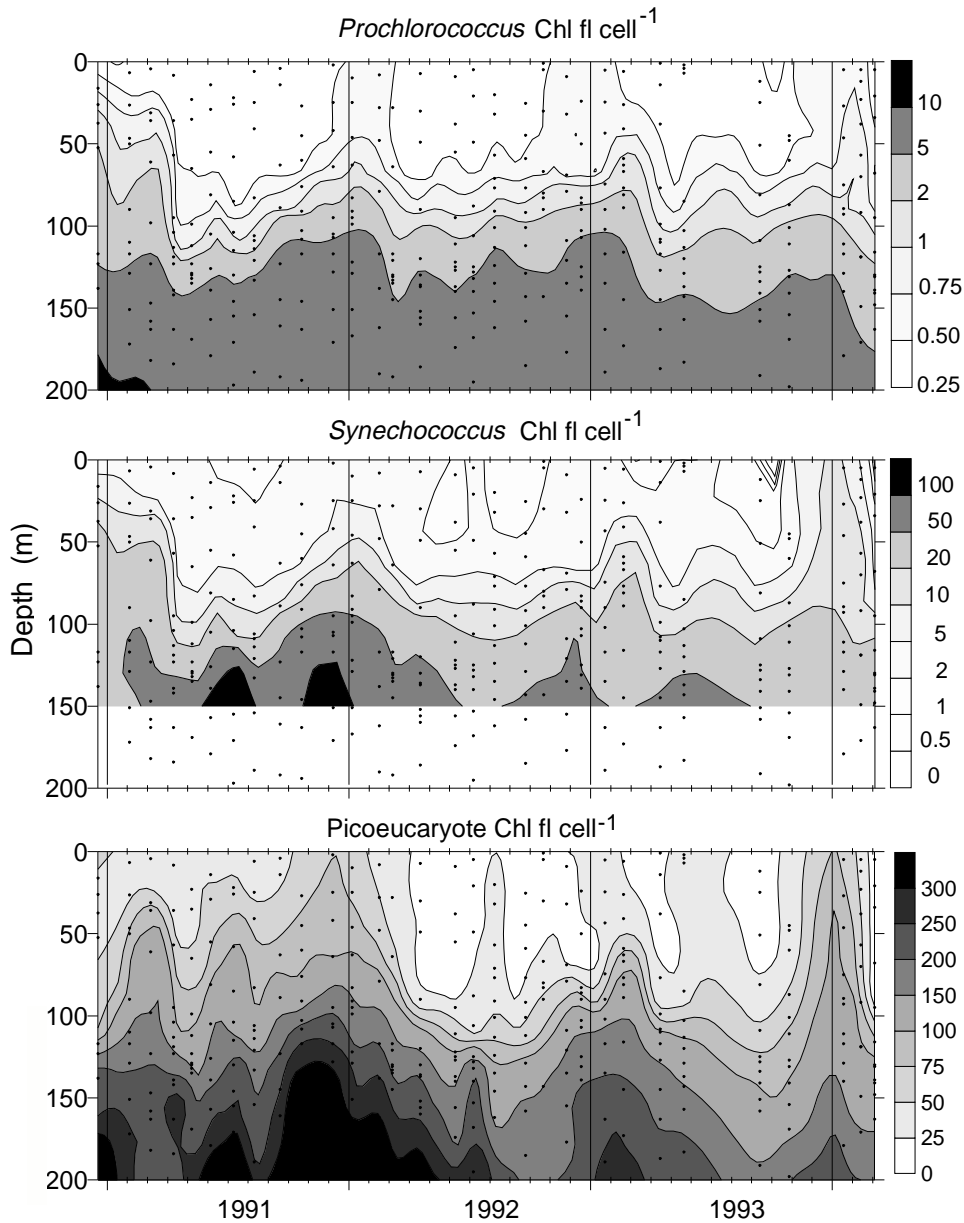


Figure 4. Time-series of relative cellular chl fluorescence for *Prochlorococcus*, *Synechococcus*, and picoeucaryotes contoured for upper 200 m from December 1990 to March 1994. Excitation was 4W all lines for *Prochlorococcus* and 1W 488nm for *Synechococcus* and picoeucaryotes. All Chl fl (680 ± 40 nm) were normalized to Fluoresbrite 0.57 μ m yellow-green standard beads (Polysciences). Sampling dates and depths are indicated by small circles posted on the contour map. Grid lines correspond to 1 January of each year.

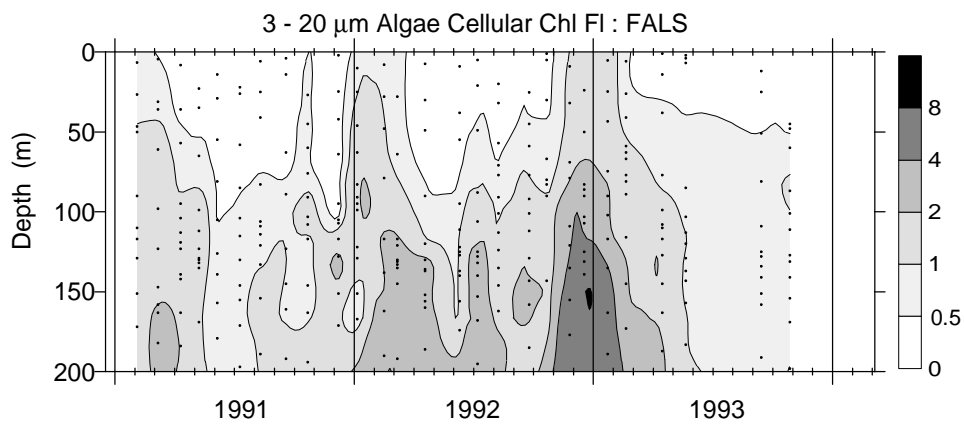


Fig. 5. Time-series of the chl fluorescence normalized to forward angle light scatter (FALS), an index of cell size. The ratio Chl : FALS for the 3 - 20 μm algae is contoured for the upper 200 m from January 1991 to October 1993. Excitation 1W 488nm, all chl fluorescence (680 \pm 40 nm) were normalized to Fluoresbrite 0.57 μm yellow-green standard beads (Polysciences). Sampling dates and depths are indicated by small circles posted on the contour. Grid lines correspond to 1 January of each year.

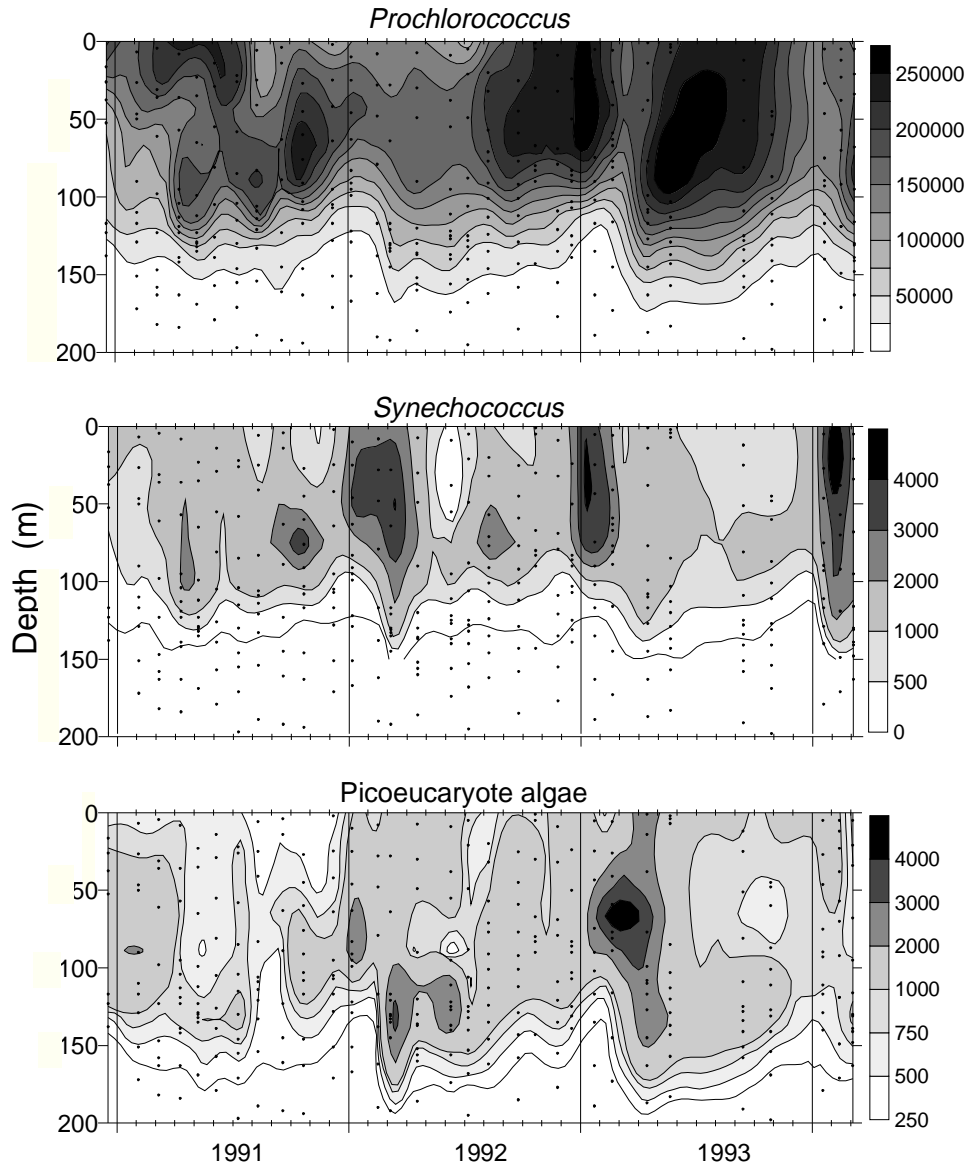


Fig. 6. Contour plots for *Prochlorococcus* abundance (cell ml⁻¹), *Synechococcus* abundance (cell ml⁻¹), and picoeucaryote abundance (cell ml⁻¹). Sampling dates and depths are indicated by small circles posted on the contour. Grid lines correspond to 1 January of each year.

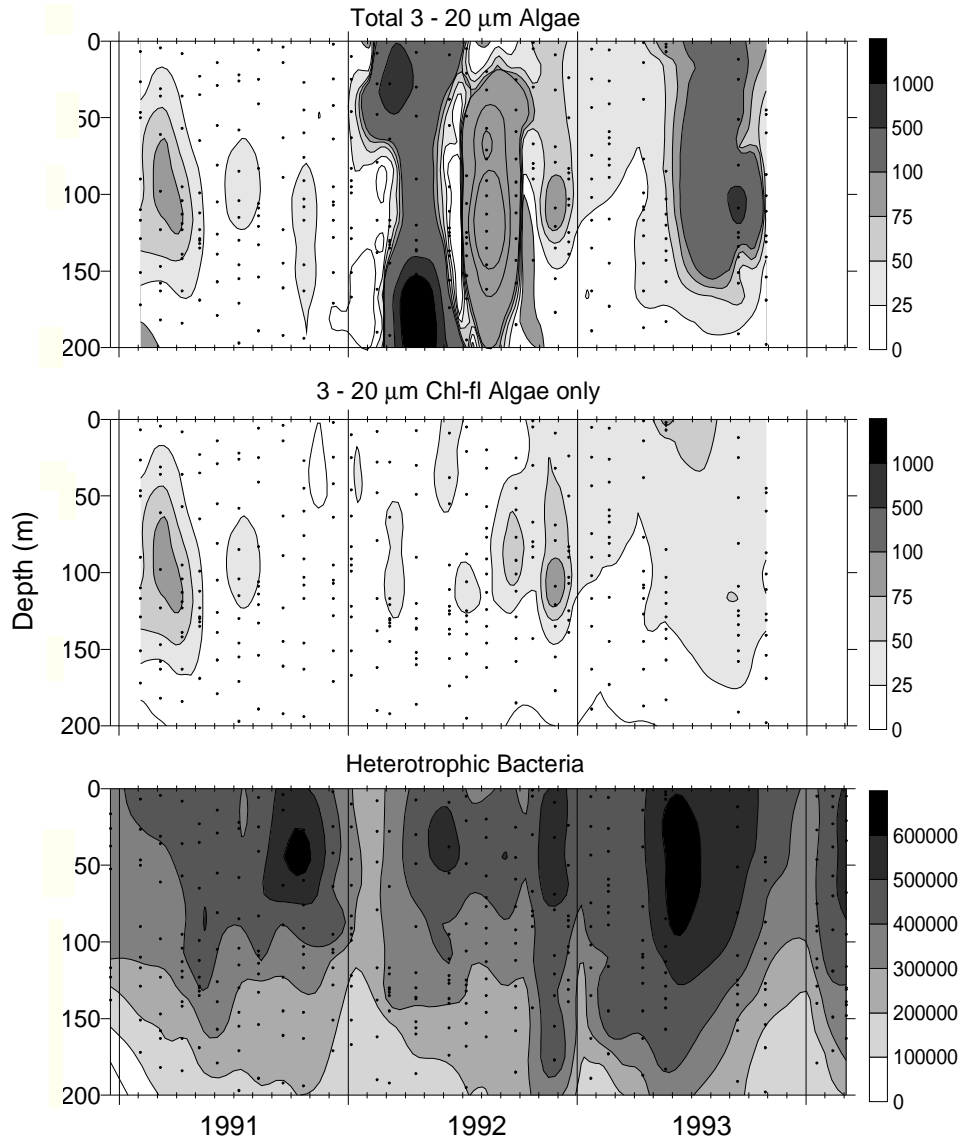


Figure 7. Contour plots for total 3–20 µm algae abundance (cell ml⁻¹), which includes both red (chl)- and orange (phycoerythrin)-fluorescing populations; Chl-fluorescing 3–20 µm algae only, from January 1991 to October 1993; and heterotrophic bacteria (cells ml⁻¹) enumerated by dual beam flow cytometry from December 1990 to March 1994. Sampling dates and depths are indicated by small circles posted on the contour. Grid lines correspond to 1 January of each year.

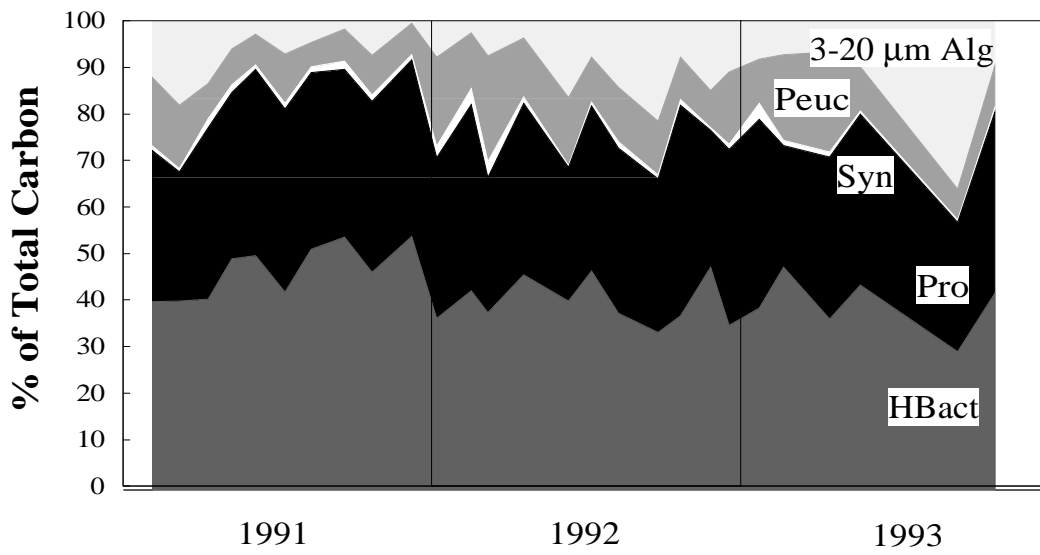


Fig. 10. *Prochlorococcus*, *Synechococcus*, picoeucaryotes, larger algae, and heterotrophic bacteria as a percentage of the total 200-m integrated estimated microbial carbon at Station ALOHA from January 1991 to October 1993.

This page intentionally left blank.

for this deeper layer (see also Winn *et al.*, 1996). The maximum increase in *Synechococcus* cellular fluorescence (taken as depth of maximum increase in cellular fluorescence between low fluorescence and high fluorescence layers) was not correlated with nitracline, mixed layer depth, or DCML; however, it was correlated with the depth of maximum increase in *Prochlorococcus* cellular fluorescence ($r = 0.85$; $p = 0.004$).

Vertical profiles of picoeucaryote cellular chl fluorescence also displayed distinct low and high cellular fluorescence layers. The increase in cellular chl fluorescence with depth was much less pronounced than for the smaller picophytoplankton, with an average of only $15 (\pm 36 \text{ SD})$ - fold increase between the low fluorescence cells of surface depths and the brighter fluorescence of cells in the high fluorescence lower layer. The depth of the subsurface abundance maximum corresponded with the depth of the high cellular chl fluorescence layer (e.g., Fig. 2) and the relationship between abundance maxima and high cellular fluorescence depths was significant for the picoeucaryotes ($r = 0.60$; $p < 0.001$), but was not for either *Prochlorococcus* or *Synechococcus*. During the Feb 1993 cruise, the shallower-than-usual large peak in picoeucaryote abundance coincided with the depth at which a rapid increase in cellular chl fluorescence was observed, and, coincidentally, the shallowest nitracline of the three-year time series (Fig. 2 and 3). The contoured time series for picoeucaryote chl fluorescence also displayed a distinct seasonal pattern with winter maxima; however, there was also considerable interannual variation in cellular fluorescence (Fig. 4). The average picoeucaryote cellular chl fluorescence was greater during the first half of our sampling period (beginning in 1991 through mid-1992) than in the latter half of the sampling period (Jul 92 - Mar 94) (Fig 4).

For the 3 - 20 μm algae, chl fluorescence per cell also increased with depth, but the vertical profile did not exhibit the 2-layer profile as for the picoplankton (Fig. 2). Instead, there was a much smaller increase with depth ($4.4 \pm 3.6 \text{ SD}$ increase), and frequently the maximum was a subsurface peak at 100 - 150 m and cellular chlorophyll fluorescence decreased below this peak. Contoured cellular fluorescence for the larger algae showed no indication of a seasonal cycle; however, if chl fluorescence is normalized to the forward angle light scatter (FALS) signal, an index of cell size for the population, winter maxima are seen (Fig. 5).

Seasonal variations

Contour plots of the 3-yr time series data for the picophytoplankton highlight a general seasonal pattern in abundance that is present throughout the euphotic zone, but is especially obvious below 100 m (Fig. 6). *Prochlorococcus* abundance varied approximately two-fold between a summer maximum and winter minimum (Fig. 6). However, in the upper 75 m, the timing of the maxima varied among years: summer to fall in both 1991 and 1993, but shifted later in 1992. For *Synechococcus*, the annual cycle difference was 3 to 4-fold, with a winter maximum (Jan - Mar) in 1992 - 1994, though the maximum was absent in 1991 (Fig. 6). For the picoeucaryotes, the maximum abundance varied 3- fold during 1991, 4-fold in 1992, and almost 6-fold in 1993. Although there appears to be considerable interannual variation in both the magnitude and the depth of the peak in abundance, the timing appears to be in the spring of each year (Fig. 6). Overall, the depth of the abundance maximum was not correlated significantly with the depth of the nitracline, but if we examine the "spring bloom" (Feb - Apr) periods only, the correlation was significant ($r = 0.93$, $p < 0.001$, $n = 9$).

The 3 - 20 μm algae included two types of cells which we could distinguish based on their fluorescence signals. The first type, eucaryotic algae with characteristic red-fluorescence due to chl *a*, were present at low abundances throughout the time series (Fig. 7). A second population of cells, which were brightly orange-fluorescing and relatively small, based on their forward angle light scatter signal, was observed intermittently. Although we did not sort this population, based on examinations of samples by epifluorescence microscopy (data not shown), we assume these cells could be the phycoerythrin-containing cyanobacteria *Synechocystis* (Ishizaka *et al.*, 1994). This population displayed considerable interannual variability, but was most abundant during 1992 and 1993 (Fig. 7). Consequently, much of the variability in the larger fraction was due to the orange-fluorescing population. The depth of the red-fluorescing algae abundance maximum occurred at approximately the same depth throughout the time series (Fig 7), whereas the orange-fluorescing cell peaks occurred at the surface and at depth (Fig. 7). Note, however, there are many fewer larger algae than picoplankton, thus counting errors are greater for this component of the phytoplankton.

For the heterotrophic bacteria, there is also an apparent seasonal cycle most obvious below 100 m; minima occur each winter. Maxima in the upper 50 m, however, occur at different times in each of the 3 years (Fig. 7). Heterotrophic bacteria abundance appeared to be correlated with *Prochlorococcus* ($r = 0.63$; $p < 0.001$).

Integrated counts for both the upper 200-m interval (Fig. 8) and the 0–50 m interval (data not shown) for each of the picophytoplankton groups also suggest a seasonal pattern. Distinct seasonal peaks were seen for *Synechococcus* and picoeucaryotes. *Synechococcus* displayed a winter peak (Jan- Mar) in both 0- 50 m and 200-m integrated abundances that was 5 - 10 times greater than the rest of the year; however, this peak was absent in 1991. For picoeucaryotes, variability among cruises was much higher than for the other picoplankton, but a 5-fold increase during spring (Mar) was observed, except in 1991. The annual cycle in *Prochlorococcus* 200-m integrated abundance was less clear. A minimum was seen each winter, but the timing of the maximum was not unique. A general increase in abundance over the sampling period was observed, and heterotrophic bacteria integrated abundance paralleled *Prochlorococcus*.

The 3–20 μm algae integrated abundance ranged over two orders of magnitude (Fig. 8). Unlike the picoplankton, there was no obvious seasonal pattern. Large peaks in abundance, especially in 1993, were due to the orange-fluorescing populations of cells (see above).

The average mixed layer depth during this time series was 50 m (± 18 m), but a seasonal peak (i.e., deepest) was detected each year in Feb (except for winter 1990/1991, when the peak was in Dec; Fig. 3). We compared the depth of the mixed layer with the vertical distributions of each picoplankton component, in particular the depths of cell abundance maxima, but there were no significant correlations. The mixed layer depth was inversely related to the peak of larger algae, but the correlation was not significant ($p = 0.08$). We next examined the relationship between the mixed layer depth and integrated abundances for all components. The most significant correlation was between the mixed layer depth and the surface (0 - 50 m) integrated *Synechococcus* abundance ($r = 0.57$; $p < 0.001$); the relationship between the 200-m integrated *Synechococcus* counts and mixed layer depth was less significant ($r = 0.45$; $p = 0.01$).

The depth of the nitracline averaged 115 m (± 19 m) and also showed a significant seasonal cycle (see also Dore and Karl, 1996). The shallowest nitracline depth occurred each winter (December) and the deepest in March/April (Fig. 3). The winter peak appeared to be related to the beginning of the *Synechococcus* maximum and *Prochlorococcus* minimum

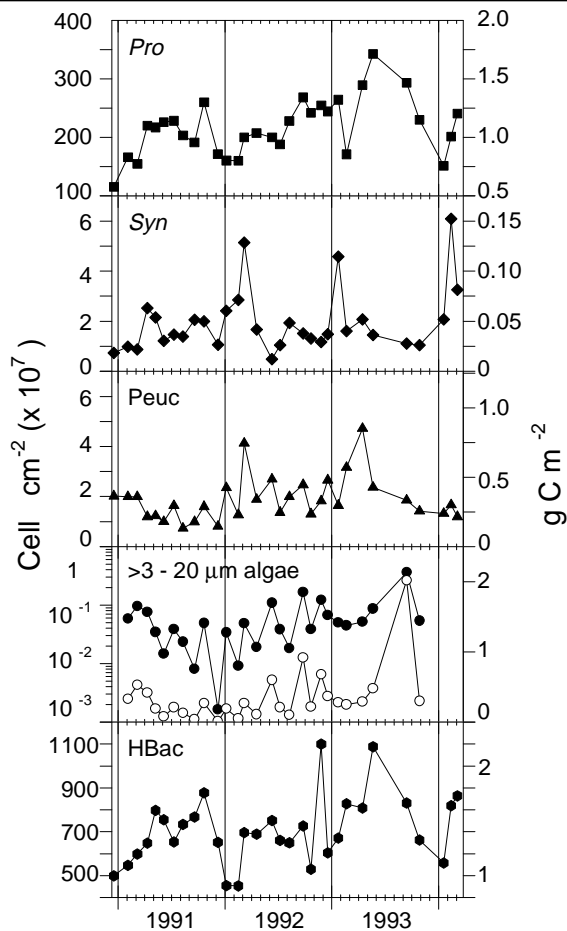


Fig. 8. The 200-m integrated abundance and carbon estimate for each component of the microbial community at Station ALOHA from December 1990 to March 1994. Note that for the 3 - 20 μm algae, abundance (\bullet) is shown on a log scale and carbon estimate (\circ) on a linear scale. Grid lines

abundance (except in 1992) (Fig. 6). Overall, the nitracline depth was only weakly correlated with the vertical distribution of each picoplankton group, except during the spring peak in picoeucaryotes (see above). Integrated 200-m water column abundances were not strongly related to the depth of the nitracline.

Interannual variations in abundance and carbon biomass

Integrated abundance for the 200-m upper water column also displayed interannual variability. In particular, the winter time maximum in abundance of *Synechococcus* and spring peak in picoeucaryotic algae were absent in 1991, but were distinctive during subsequent winters (Fig. 8). Estimated carbon biomass increased for each of the groups during the time series (Table 1). Significant increases were seen in *Prochlorococcus* 200-m integrated abundance and carbon biomass; the 1993 monthly average was significantly greater than 1991 ($p = 0.038$). For the 3–20 μm algae, integrated total counts in the

Table 1. Interannual differences in the mean, SD, minimum and maximum 200-m integrated carbon estimates for *Prochlorococcus*, *Synechococcus*, <3 μm picoeucaryote algae, 3 - 20 μm algae, heterotrophic bacteria, and total microbial carbon at Station ALOHA. Results are based on data from cruises between Dec 1990 and Mar 1994 ($n = 31$) using carbon conversion factors as in Campbell *et al.* (1994).

Component	Number of cruises	200-m Integrated Carbon Estimates (g C m ⁻²)			
		1991	1992	1993	1990-1994 Overall mean
		10	11	6	31
<i>Prochlorococcus</i>	Mean	1.04	1.13	1.41	1.14
	SD	0.22	0.19	0.31	0.26
	Min	0.61	0.61	0.91	0.61
	Max	1.38	1.42	1.82	1.82
<i>Synechococcus</i>	Mean	0.04	0.05	0.05	0.05
	SD	0.02	0.03	0.03	0.03
	Min	0.02	.01	0.03	0.01
	Max	0.06	0.13	0.11	0.13
Picoeucaryote algae	Mean	0.28	0.44	0.51	0.38
	SD	0.10	0.17	0.25	0.18
	Min	0.15	0.26	0.29	0.15
	Max	0.41	0.84	0.95	0.95
>3 - 20 μm algae	Mean	0.20	0.34	0.60	0.31
	SD	0.17	0.28	0.70	0.30
	Min	0.01	0.05	0.25	0.01
	Max	0.53	0.92	2.02	2.02
Heterotrophic bacteria	Mean	1.37	1.33	1.63	1.42
	SD	0.23	0.35	0.31	0.31
	Min	1.00	0.91	1.32	0.91
	Max	1.75	2.20	2.18	2.20
Total	Mean	2.92	3.32	4.20	3.30
	SD	0.45	0.76	0.99	0.82
	Min	2.03	2.13	3.16	2.03
	Max	3.78	4.63	5.64	5.64

0–50 m interval also increased significantly during this time series ($p = 0.002$). The largest peak for the 3–20 μm component was seen in 1993, and was due predominately to the orange-fluorescing cells (Fig. 8). The total estimated microbial carbon (*Prochlorococcus* + *Synechococcus* + picoeucaryotes + larger algae + heterotrophic bacteria) increased significantly from an average of 2.92 mg C m⁻² in 1991 to 4.20 mg C m⁻² in 1993 ($p = 0.002$) (Fig. 9 and Table 1).

When the contribution of each component is plotted as a percentage of the total estimated microbial carbon, the overall dominance of the procaryotic biomass is obvious (Fig. 10), as has been reported previously (Fuhrman *et al.*, 1989; Campbell *et al.*, 1994; Li 1995). During this time series, the heterotrophic bacteria contributed from 30–54 % of the total integrated 200-m water column microbial carbon. The percentage contributed by heterotrophic bacteria decreased from an average of 47 % in 1991 to 40 % in 1992 and 1993, in spite of an overall increase in estimated carbon biomass (Table 1). The average *Prochlorococcus* contribution

Total Microbial Carbon Estimate and the SOI

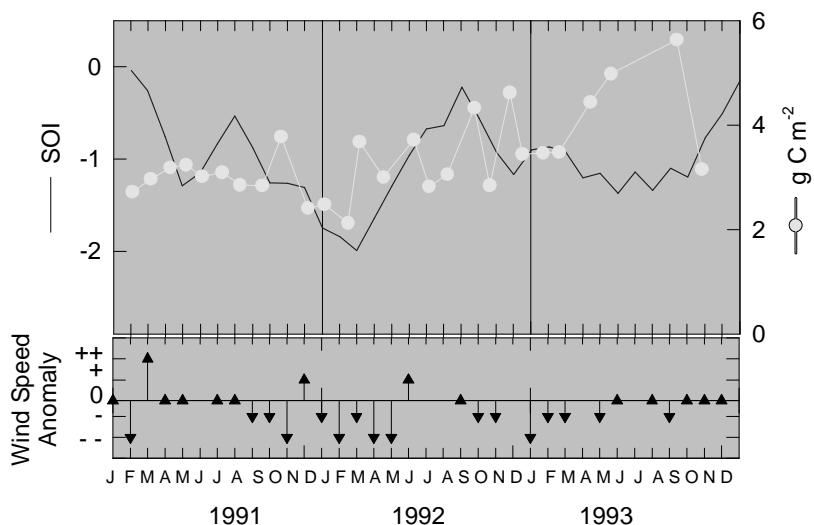


Figure 9. Upper panel: Estimated total microbial carbon biomass (\bullet) and the 3-month running mean for the Southern Oscillation Index (SOI) (—) from Jan 1991 - Dec 1993. Total biomass is the sum of *Prochlorococcus* + *Synechococcus* + picoeucaryotes + 3 - 20 μm algae + heterotrophic bacteria carbon biomass. The 1991-1994 ENSO event began in Mar 91, indicated by a negative SOI, and continued throughout this time series, except for a short weakening during April-July 1992. Lower panel: Wind speed anomalies (departures from 23 year monthly mean [1961-1983]) around Station ALOHA from Jan 1991 to Dec 1993 are plotted on a scale from -- to ++ (B. Wang, pers. commun.), where -- = much weaker than normal ($< -1 \text{ m s}^{-1}$ anomaly); - = slightly weaker than normal (0 to -1 m s^{-1} anomaly); 0 indicates normal conditions (NE trade winds); + = slightly stronger than normal (0 to 1 m s^{-1} anomaly); ++ = much stronger than normal ($> 1 \text{ m s}^{-1}$ anomaly). Data from J. O'Brien and J. Stricherz in the *Climate Diagnostic Bulletin* published by NOAA/NWS/NCEP.

(34 - 35 %) was similar in each year, as was *Synechococcus*, which was a very small percentage of the total (Tables 1 & 2). The picoeucaryotes and larger algae components were highly variable within each year, but together contributed a larger percentage of the estimated carbon biomass in the latter half of the time series (Fig. 10).

Prochlorococcus dominance of the microbial carbon biomass is limited to the upper portion of the euphotic zone (SML; Table 2). The contribution of heterotrophic bacterial biomass increases with depth and is the major contributor below the DCML. The contribution from picoeucaryotes is largest at the DCML, and the 3-20 μm algae contribution is 7-10 % throughout the euphotic zone (Table 2).

DISCUSSION

The perception of open ocean central gyres as a stable, homogeneous environment on both temporal and spatial scales is changing as the result of the extensive time series data now available (e.g. Hawaii Ocean Time-series (HOT) and Bermuda Atlantic Time-Series (BATS)). Previously, the inability to detect seasonal cycles in phytoplankton biomass as predicted from simple models (e.g. Cushing, 1959) was likely due to under-sampling (see Winn *et al.*, 1996). For the subtropical central North Pacific, recent observations from the

Table 2. The average percentage of carbon biomass (± 1 SD) contributed by each component of the community for December 1990–March 1994 ($n = 31$) for the 200-m water column, the surface mixed layer (SML), the deep chlorophyll maximum layer (DCML), and below the DCML layer (Deep). Overall ratio of photosynthetic biomass: HBac is 56:44. An average total carbon estimate (mg C m^{-3}) for each depth stratum was calculated by dividing the integrated total C estimate by the depth of the interval.

Component	Water Column	SML	DCML	Deep
	0–200 m (%)	0–50 m (%)	114 \pm 18 m (%)	120–175 m (%)
<i>Prochlorococcus</i>	35.1 (5)	42.0 (6)	26.0 (9)	14.5 (5)
<i>Synechococcus</i>	1.6 (1)	2.2 (1)	0.01 (1)	0.2 (0.4)
Picoeucaryotic algae	11.6 (5)	9.3 (4)	18.3 (6)	13.2 (6)
3 - 20 mm Algae	8.1 (8)	7.4 (8)	10.1 (9)	10.4 (11)
Heterotrophic bacteria	43.6 (6)	39.9 (7)	46.2 (11)	62.7 (11)
Average Total Carbon for each interval (mg C m^{-3})	16.5	23.4	13	12

time series at Station ALOHA reveal variability on both seasonal and interannual time scales (e.g., Letelier *et al.*, 1993; Karl *et al.*, 1995).

Seasonal variations in community structure

Patterns of temporal variability in the larger phytoplankton in the central North Pacific Ocean have been reported by Venrick (1993). She identified two groups of species within the phytoplankton ($> 5 \mu\text{m}$) that could be defined by the depth and timing of their maximum frequency of occurrence. During the summer, the surface species were found most frequently in the upper 75 m. The deep species (75 - 150 m) bloomed in winter. This distinct vertical structure was observed consistently, but because the timing of the maxima in these two groups did not coincide, Venrick suggested that a seasonal cycle in biomass would be masked.

Different phasing in seasonal cycles may exist for the picophytoplankton in the subtropical North Pacific as well. The relatively small range of variation in cell abundance (Fig. 2) and in 200-m integrated abundance (especially for *Prochlorococcus*) is consistent with our previous report for the picophytoplankton based on only four profiles (Campbell and Vault, 1993). From this 3-yr time series, however, we can identify a seasonal pattern in the abundance of the autotrophic components, though there is considerable interannual variability as well.

The suggested phasing in the peaks of abundance for each of the picophytoplankton (i.e., *Synechococcus* in winter, picoeucaryotes in spring, *Prochlorococcus* in late summer/fall) corresponds to what we would predict based on our knowledge of these groups (e.g., Olson *et al.*, 1990; Blanchot *et al.*, 1992). Decreased water column stability and increased nitrate stimulate *Synechococcus*. Observed peaks in *Synechococcus* follow the occurrence of the deepest mixed layer depths (December–February) and the shoaling of the nitracline (Figs 3, 6, and 8). The depth of the mixed layer, although not strongly correlated with abundance of any component, was significantly correlated with *Synechococcus* 200-m integrated counts.

Our findings are consistent with observations in the Mediterranean Sea, where peaks in *Synechococcus* occurred after mixing, in a less stable water column, and *Prochlorococcus* occurred only under stratified conditions (Bustillos-Guzmán *et al.*, 1995). At Station ALOHA, the annual cycle in *Prochlorococcus* abundance appears to coincide with periods of shallow mixed layer depth (Figs. 3, 6, 8). The extension of the summer/fall *Prochlorococcus* “peak” through winter of 1992/93 (Fig. 6) occurred during a period of very shallow mixed layer depths (Fig. 3). The *Prochlorococcus* annual cycle is also related to the seasonal pattern in the depth of nitracline, and, therefore, the availability of nutrients. During 1991 and 1993, the maximum in *Prochlorococcus* occurred when the nitracline was deepest, at which time *Prochlorococcus* may outcompete other algae, or, perhaps, is more efficient at utilizing recycled nutrients. This pattern was not evident for *Prochlorococcus* during 1992, however.

The bloom of picoeucaryotes during spring is coincident with the temporal distributions of pigment concentrations at the DCML at Station ALOHA, in particular 19'-hexanoyloxyfucoxanthin and 19'-butanoyloxyfucoxanthin (Letelier *et al.*, 1993). These two pigments are diagnostic markers for prymnesiophytes and pelagophytes, respectively, which have been shown to be dominant picoeucaryotes at Station ALOHA (Andersen *et al.*, 1996). Spring time increases in chl *a* at the DCML were shown to be due to an increase in the daily average irradiance combined with an increase in nutrient supply resulting from vertical displacement of the pycnocline (Letelier *et al.*, 1993). Recent observations in the Gulf of Aqaba, Red Sea, however, revealed a different pattern in succession which began with the picoeucaryotes in winter (Lindell and Post, 1995). Most likely, this difference is due to very different hydrographic conditions (e.g. mixing to 600 m). Also, the winter nutrient-replete conditions included measurable nitrate in surface waters, a situation which never occurred at Station ALOHA.

The seasonal variations in picophytoplankton community structure we observed are similar to other regions of the ocean. In the North Atlantic at Station OFP (Sargasso Sea), the summer peak in *Prochlorococcus* alternates with a winter (February) peak in *Synechococcus*, and the magnitude of the seasonal changes for each component are not much different from what we have found at Station ALOHA: in summer, a 3-fold increase for integrated *Prochlorococcus* abundance; in winter (Feb), a 5-fold increase for *Synechococcus*, and an approximately 2-fold increase for picoeucaryotes (Olson *et al.*, 1990). The absolute abundances of the picophytoplankton, however, are very different. At Station ALOHA (22° N), *Prochlorococcus* always exceeds *Synechococcus* by two orders of magnitude, whereas at Station OFP (31° N) *Synechococcus* abundance equals *Prochlorococcus* during its winter peak, and is only 10- to 20- fold lower during summer. This difference could be due to either latitudinal differences in community structure or differences between oceans. Shifts in community composition were observed along a transect through tropical, subtropical and subarctic latitudes in the Atlantic Ocean during summer 1993 (Buck *et al.*, 1996). A comparison of Station ALOHA summer integrated abundances with the 20° N Atlantic station reveals equivalent abundances of picoplankton (Buck *et al.*, 1996). Thus, it appears that while latitudinal differences occur, the community structure in the Pacific is similar to the Atlantic at 20° N.

At a station 10 km off Japan (35° N; 1000 m), *Prochlorococcus* also exhibited a seasonal pattern, with an abundance maximum in July - Oct. (Shimada *et al.*, 1995). Because maximum integrated abundances of both *Synechococcus* and *Prochlorococcus* coincided in September, when water temperature exceeded 20° C, it appeared that temperature, rather

than water column stability, was the limiting factor for both populations at this coastal station.

Cellular chlorophyll fluorescence

As reported previously for the picophytoplankton at Station ALOHA, fluorescence per cell for all groups increased with depth (Campbell and Vaultot 1993). For the picoplankton, the large increase in cellular chl fluorescence observed with depth in the water column could be due to (1) a small package effect because of their small size; (2) photoacclimation, e.g., a change in the Chl *a* : Chl *b* ratio for *Prochlorococcus* (Veldhuis and Kraay, 1990; Moore *et al.* 1995); (3) changes in quantum yield; and/or (4) shifts in population composition. For the 3–20 μm algae, the difference between surface and maximum cellular chl fluorescence was much smaller than for picoplankton. This difference is most likely due to the greater impact of packaging effect and to physiological differences resulting in a lower capacity to photoacclimate for the larger algae.

A significant seasonal cycle was evident in cellular chlorophyll fluorescence for each of the autotrophic components, with maxima occurring each winter (Fig. 4). The two-fold annual variation in cellular chl fluorescence was less than the five-fold increase measured for picoplankton in the North Atlantic (Olson *et al.*, 1990). Nevertheless, the observed winter maximum was also hypothesized to be a photoadaptive response to the reduced average light intensity to which cells are exposed in winter because of the deeper mixed layer (Winn *et al.*, 1996). Our data for cellular chl fluorescence for all the picophytoplankton (Fig. 4), as well as the chl fluorescence normalized to size (Chl:FALS) for the 3–20 μm algae (Fig. 5), support this hypothesis. For *Prochlorococcus* the coefficient of variation for mean cellular chl fluorescence increased during winter. If deeper populations are mixed up into surface waters during winter, we would expect to see a greater range in cellular fluorescence within a sample, which would result in more variation around the mean.

For the picoeucaryotes, cellular chl fluorescence varied on an interannual scale as well (Fig. 4). Cellular chl fluorescence during the first half of the time series (Dec 1990 - Mar 1992) was significantly higher than in the latter half of the time series (t-test; $p < 0.004$); however, light scatter (both forward angle and right angle light scatter parameters) were not significantly different for the picoeucaryotes between these time periods. This shift may have been due to different species composition, or changing nutrient conditions of the ongoing ENSO event.

Interannual Variations

Global climate variations, such as those resulting from ENSO, have been shown to affect phytoplankton community structure in the equatorial Pacific (Blanchot *et al.*, 1992). Karl *et al.* (1995) have suggested that the ENSO event beginning in 1991 had a marked effect on the ecosystem structure and productivity at Station ALOHA in the upper 50 m. One of the principal effects seen during 1991- 1993 was increased water column stability, which resulted in a change in phytoplankton community composition. In particular, this event produced conditions favorable for *Trichodesmium* growth. Although they estimated *Trichodesmium* was a small component of the biomass, it was predicted to make a significant input of fixed nitrogen to the surface mixed layer (Karl *et al.*, 1995). One possible outcome of nitrogen fixation by *Trichodesmium* is that excess nitrogen is then available for other organisms, e.g.

an echo bloom. If the excess nitrogen stimulates picophytoplankton, this could result in a shift in the phytoplankton community composition, as was predicted from the observed increase in assimilation number (Karl *et al.*, 1995). Picoeucaryotes have been observed to make the largest contribution to primary production in oceanic regions (e.g., Li 1994). Such an increase in picophytoplankton production would be consistent with the decrease in export production observed during this ENSO event (Karl *et al.*, 1996). Community structure and composition have been shown to be important factors in the coupling between production of organic carbon in surface waters and flux of particulate carbon to the deep ocean (Longhurst and Harrison, 1989; Michaels and Silver, 1988). In the North Atlantic Bloom experiment, algal cell size was the primary explanation for the interannual difference in observed fluxes (Boyd and Newton, 1995).

The prevailing winds in the region of Station ALOHA normally are northeast trades; however, during this three-year period (1991 - 1993), the winds were overall much weaker (Fig. 9). Weaker than normal trade winds (Fig. 9) and, consequently, more stable water column conditions associated with the 1991-1994 ENSO event may have influenced the community structure and composition at Station ALOHA (e.g., Karl *et al.*, 1995). This event, which began in Mar 1991 as the Southern Oscillation Index (SOI) decreased (Fig. 9), was considerably longer than average (McPhaden, 1993). It strengthened throughout 1991, until a slacking off in Apr - Jul 1992, but then intensified in Oct - Dec 1992. For the microbial community, the interannual variability superimposed on the annual patterns we have observed may be related to the extended duration of this ENSO event. The total estimated microbial carbon integrated for the upper 200-m at Station ALOHA increased during our three-year time series observations (Table 1). Similar increases were seen for the 0-50 m interval as well. Within each year, biomass estimates for each component fluctuated two- to several-fold (Fig. 8), but overall the largest effects were seen in the biomass estimates for the eucaryotic algae. Picoeucaryote biomass almost doubled and the >3- 20 μm algae tripled during this period (Table 1).

Additional data are needed to further examine the variability in community structure and biomass estimates during "normal" conditions. In particular, data collected at more frequent intervals (e.g., moored instruments; Dickey, 1988), will be necessary to investigate the sources of physical variability further and to examine the responses of phytoplankton to such events.

CONCLUSIONS

Prochlorococcus is a dominant and consistent component of the phytoplankton at Station ALOHA. Abundance minima occur each winter as water column stability decreases, and abundance maxima may occur during summer/fall, when *Prochlorococcus* apparently can outcompete other algae. Peaks in *Synechococcus* occurred in winter, typically when the mixed layer was deeper and the nitracline shallower; nevertheless, *Synechococcus* was never a large percentage of the biomass (Fig. 10). Picoeucaryote algae abundance maxima occurred in spring. Integrated abundance of picoeucaryotes displayed considerable variability within and among years (Fig 8 and Table 1). During the latter half of the time series, a possible shift in species composition of the picoeucaryotes was shown by a decrease in average cellular fluorescence coincident with an increase in cell abundance. The 3-20 μm algae displayed the greatest spatial and temporal variability in abundance and in contribution to the total estimated microbial biomass. Weaker than normal trade winds

(Fig. 9), as well as the more stable water column conditions associated with the developing 1991-1994 ENSO, event may have contributed to interannual variability in community composition.

The apparent succession of seasonal cycles, along with the considerable interannual variability, for both the picoplankton and larger algae, as well the coincidence of winter maxima in cellular chlorophyll for each of these groups in the upper euphotic zone as the result of photoacclimation (see also Winn *et al.*, 1996), may explain why an annual pattern in phytoplankton biomass has been difficult to establish for the subtropical North Pacific Ocean.

Acknowledgments— We thank J. Christian, J. Dore, D. Hebel, T. Houlihan, D.M. Karl, R. Letelier, U. Maggaard, G. Tien, L. Tupas, and C. Winn of the HOT, and S. Chiswell and R. Lukas and WOCE programs for their continuous generous support of this project, and G. Castro for help in the laboratory. We thank D.M. Karl, R. Scharek, E. Venrick and two anonymous reviewers for comments on the manuscript, and B. Wang for discussions on climatological data. We acknowledge a grant from the National Science Foundation OCE 90-15883 to L. C. for support of this research. This is JGOFS contribution No. 288.

REFERENCES

- Andersen R. A., Bidigare R. R., Keller M. D. and Latasa M. (1996) A comparison of HPLC pigment signatures and electron microscopic observations for oligotrophic waters of the North Atlantic and Pacific Oceans. *Deep-Sea Research II*, **43**, 517-537.
- Bienfang P. K. and Szyper J. P. (1981) Phytoplankton dynamics in the subtropical Pacific Ocean off Hawaii. *Deep-Sea Research*, **28A**, 981-1000.
- Blanchot J., Rodier M. and Le Bouteiller A. (1992) Effect of El Niño Southern Oscillation events on the distribution and abundance of phytoplankton in the western Pacific Tropical Ocean along 165°E. *Journal of Plankton Research*, **14**, 137-156.
- Boyd P. and Newton P. (1995) Evidence of the potential influence of planktonic community structure on the interannual variability of particulate organic carbon flux. *Deep-Sea Research*, **42**, 619-639.
- Buck K. R., Chavez F. P. and Campbell L. (1996) Basin-wide distributions of living carbon components and the inverted trophic pyramid of the central gyre of the north Atlantic Ocean, summer 1993, *Aquatic Microbial Ecology*, **10**, 283-298.
- Bustillos-Guzmán J., H. Claustre and J.-C. Marty (1995) Specific phytoplankton signatures and their relationship to hydrographic conditions in the coastal northwestern Mediterranean Sea. *Marine Ecology Progress Series*, **124**, 247-258.
- Campbell L. and D. Vaulot (1993) Photosynthetic picoplankton community structure in the subtropical North Pacific Ocean near Hawaii (Station ALOHA). *Deep-Sea Research*, **40**, 2043-2060.
- Campbell L., H. A. Nolla and D. Vaulot (1994) The importance of *Prochlorococcus* to community structure in the central North Pacific Ocean. *Limnology and Oceanography*, **39**, 954-961.
- Cushing J. D. (1959) The seasonal variation in oceanic production as a problem in population dynamics. *J. Cons. Int. Explor. Mer.*, **24**, 455-464.
- Dickey T. D. (1988) Recent advances and future directions in multi-disciplinary *in situ* oceanographic measurement systems. In: *Toward a theory on biological-physical interactions in the world ocean*, B. J. Rothschild, editor, Kluwer Academic Publishers, Dordrecht, pp. 555-598.
- DiTullio G. R. and E. A. Laws (1991) Impact of an atmospheric-oceanic disturbance on phytoplankton community dynamics in the North Pacific central gyre. *Deep-Sea Research*, **38**, 1305-1329.
- Dore J. E. and D. M. Karl (1996) Nitrite distributions and dynamics at Station ALOHA. *Deep-Sea Research II*, **43**, 385-402.
- Fuhrman J. A., T. D. Sleeter, C. A. Carlson and L. M. Proctor (1989) Dominance of bacterial biomass in the Sargasso Sea and its ecological implications. *Marine Ecology Progress Series*, **57**, 207-217.
- Hayward T. L., E. L. Venrick and J. A. McGowan (1983) Environmental heterogeneity and plankton community structure in the central North Pacific. *Journal of Marine Research*, **41**, 711-729.

- Ishizaka J., H. Kiyosawa, K. Ishida, K. Ishikawa and M. Takahashi (1994) Meridional distribution and carbon biomass of autotrophic picoplankton in the Central North Pacific during late Northern summer 1990. *Deep-Sea Research*, **41**, 1745-1766.
- Karl D. M. and C. D. Winn (1991) A sea of change: monitoring the oceans' carbon cycle. *Environmental Science and Technology*, **25**, 1977-1981.
- Karl D. M., R. M. Letelier, D. Hebel, L. Tupas, J. Dore, J. Christian and C. Winn (1995) Ecosystem changes in the North Pacific subtropical gyre attributed to the 1991-1992 El Niño. *Nature*, **373**, 230-234.
- Karl D. M., J. R. Christian, J. E. Dore, D. V. Hebel, R. M. Letelier, L. M. Tupas and C. D. Winn (1996) Seasonal and interannual variability in primary production and particle flux at Station ALOHA. *Deep-Sea Research II*, **43**, 539-568.
- Lepesteur M., J. M. Martin and S. Fleury (1993) A comparative study of different preservation methods for phytoplankton cell analysis by flow cytometry. *Marine Ecology Progress Series*, **93**, 55-63.
- Letelier R. M., R. R. Bidigare, D. V. Hebel, M. Ondrusek, C. D. Winn and D. M. Karl (1993) Temporal variability of phytoplankton community structure based on pigment analysis. *Limnology and Oceanography*, **38**, 1420-1437.
- Letelier R. M., J. E. Dore, C. D. Winn and D. M. Karl (1996) Seasonal and interannual variations in photosynthetic carbon assimilation at Station ALOHA. *Deep-Sea Research II*, **43**, 467-490.
- Li W. K. W. (1994) Primary production of prochlorophytes, cyanobacteria, and eucaryotic ultraphytoplankton: Measurements from flow cytometric sorting. *Limnology and Oceanography*, **39**, 169-175.
- Li W. K. W. (1995) Composition of ultraphytoplankton in the central North Atlantic. *Marine Ecology Progress Series*, **122**, 1-8.
- Lindell D. and A.F. Post (1995) Ultraphytoplankton succession is triggered by deep winter mixing in the Gulf of Aqaba (Eilat), Red Sea. *Limnology and Oceanography*, **40**, 1130-1141.
- Longhurst A. R. and W. G. Harrison (1989) The biological pump: profiles of plankton production and consumption in the upper ocean. *Progress in Oceanography*, **22**, 47-123.
- McGowan J. A. and T. L. Hayward (1978) Mixing and oceanic productivity. *Deep-Sea Research*, **25**, 771-793.
- McPhaden M.J. (1993) TOGA-TAO and the 1991-93 El Niño-Southern Oscillation event. *Oceanography*, **6**, 36-44.
- Michaels A. F. and M. W. Silver (1988) Primary production, sinking fluxes and the microbial food web. *Deep-Sea Research*, **35**, 473-490.
- Moore, L. R., R. Goericke, and S.W. Chisholm (1995) Comparative physiology of *Synechococcus* and *Prochlorococcus*: influence of light and temperature on growth, pigments, fluorescence and absorptive properties. *Marine Ecology Progress Series*, **116**, 259-275.
- Olson R. J., E. R. Zettler and K. O. Anderson (1989) Discrimination of eukaryotic phytoplankton cell types from light scatter and autofluorescence properties measured by flow cytometry. *Cytometry*, **10**, 636-643.
- Olson R. J., S. W. Chisholm, E. R. Zettler, M. A. Altabet and J. A. Dusenberry (1990) Spatial and temporal distributions of prochlorophyte picoplankton in the North Atlantic Ocean. *Deep-Sea Research*, **37**, 1033-1051.
- Shimada A., M. Nishijima and T. Maruyama. 1995. Seasonal appearance of *Prochlorococcus* in Suraga Bay, Japan in 1992-1993. *Journal of Oceanography*, **51**, 289-300.
- Simon, N., R.G. Barlow, D. Marie, F. Partensky and D. Vaultot. 1994. Characterization of oceanic photosynthetic proeukaryotes by flow cytometry. *Journal of Phycology*, **30**, 922-935.
- Tupas L., F. Santiago-Mandujano, D. Hebel, E. Firing, F. Bingham, R. Lukas and D. Karl. 1994. Hawaii Ocean Time-series Data Report 5. 1993. SOEST Technical Report 94-5.
- Tupas L., F. Santiago-Mandujano, D. Hebel, E. Firing, R. Lukas, and D. Karl. 1995. Hawaii Ocean Time-series Data Report 6: 1994. SOEST Technical Report 95-6.
- Tupas L., F. Santiago-Mandujano, D. Hebel, R. Lukas, D. Karl and E. Firing. 1993. Hawaii Ocean Time-series Data Report 4. 1992. SOEST Technical Report 93-14.
- Vaultot D. (1989) CYTOPC: processing software for flow cytometric data. *Signal and Noise*, **2**, 8.
- Vaultot D., C. Courties and F. Partensky (1989) A simple method to preserve oceanic phytoplankton for flow cytometric analyses. *Cytometry*, **10**, 629-635.
- Vaultot D., D. Marie, R. J. Olson and S. W. Chisholm (1995) Growth of *Prochlorococcus*, a photosynthetic prokaryote, in the Equatorial Pacific ocean. *Science*, **268**, 1480-1482.
- Veldhuis M. J. W. and G. W. Kraay (1990) Vertical distribution and pigment composition of a picoplanktonic prochlorophyte in the subtropical North Atlantic: a combined study of HPLC- analysis of pigments and flow cytometry. *Marine Ecology Progress Series*, **68**, 121-127.

- Venrick E. L. (1993) Phytoplankton seasonality in the central North Pacific: the endless summer reconsidered. *Limnology and Oceanography*, **38**, 1135-1149.
- Venrick E. L., J. A. McGowan, D. R. Cayan and T. L. Hayward (1987) Climate and chlorophyll *a*: long-term trends in the Central North Pacific Ocean. *Science*, **238**, 70-72.
- Wang B. (1995) Interdecadal changes in El Niño onset in the last four decades. *Journal of Climate*, **8**, 267-285.
- Winn C. D., L. Campbell, J. R. Christian, R. M. Letelier, D. V. Hebel, J. E. Dore, L. Fujieki and D. M. Karl (1996) Seasonal variability in the phytoplankton community of the North Pacific Subtropical Gyre. *Global Biogeochemical Cycles*, **9**, 605-620.
- Winn C. D., R. Lukas, D. M. Karl and E. Firing. 1993. Hawaii Ocean Time-series Data Report 3. 1991. SOEST Technical Report 93-3.
- Zweifel, U.L. and A. Haagstrom (1995) Total counts of marine bacteria include a large fraction of non-nucleoid-containing bacteria (ghosts). *Applied and Environmental Microbiology*, **61**, 2180-2185.